ELSEVIER

Journal of Alloys and Compounds 293–295 (1999) 521–525

Journal of ALLOYS AND COMPOUNDS

Improvement of hydrogen storage properties of melt-spun Mg–Ni–RE alloys by nanocrystallization

Kazuhide Tanaka[a,*], Yoshisada Kanda[a], Masaki Furuhashi[a], Katsushi Saito[b], Kotaro Kuroda[b], Hiroyasu Saka[b]

[a]*Department of Materials Science and Engineering, Nagoya Institute of Technology, Showa-ku, Nagoya 466, Japan*
[b]*Department of Quantum Engineering, Nagoya University, Nagoya 464-01, Japan*

Abstract

The hydrogen absorbing rates and pressure–composition isotherms (*PCT*) are measured on Mg–Ni and Mg–Ni–RE (RE=La, Nd) alloys which have been amorphized by melt-spinning and crystallized to form nanocrystalline structures. The microstructures of these alloys as examined by X-ray diffraction and transmission electron microscopy consist of mixtures of crystalline grains of major Mg and Mg_2Ni phases, together with a minor La_2Mg_{17} or $NdMg_{12}$ phase, of 50–100 nm in diameter. These nanocrystallized alloys, particularly of the Mg–Ni–RE systems, exhibit excellent hydrogen absorbing kinetics and *PCT* characteristics in comparison with those of the corresponding as-cast alloys with coarse eutectic structures.

Keywords: Mg–Ni–RE alloys; Melt-spinning; Nanocrystallization; Hydrogen absorption rate; Pressure–composition isotherm

1. Introduction

The hydrogen absorbing and desorbing rates of Mg-based alloys are strongly influenced not only by their surface conditions but also by microstructures. In as-cast materials, which often exhibit coarse eutectic structures of primary (Mg) and secondary intermetallic phases, the initial absorbing rate is quite small and many hydriding–dehydriding cycles are required to attain a complete activation. However, by refining the microstructures, the activation behavior may be considerably improved. In our study of hydrogen absorption in Mg-rich Mg–Ni and Mg–Ni–RE (RE=La, Nd) alloys, it has been found that the absorbing rate is much enhanced by nanocrystallization [1]. The nanostructure can be obtained by crystallizing amorphous alloys produced by melt-spinning. Through this treatment materials with grain sizes of 50–100 nm are readily obtained, for which the complete activation can be attained after a few cycles. In this paper, the hydrogen absorbing behavior and *PCT* characteristics, as well as TEM observations, of these materials are presented and the effect of nanostructure on the hydrogen absorption is discussed.

2. Experimental

Fig. 1 shows an equilibrium phase diagram of the Mg–Ni system [2], where the glass-forming ranges with and without additional RE elements are included. With the addition of 5% La or Nd, the glass-forming range is significantly extended. Binary and ternary amorphous

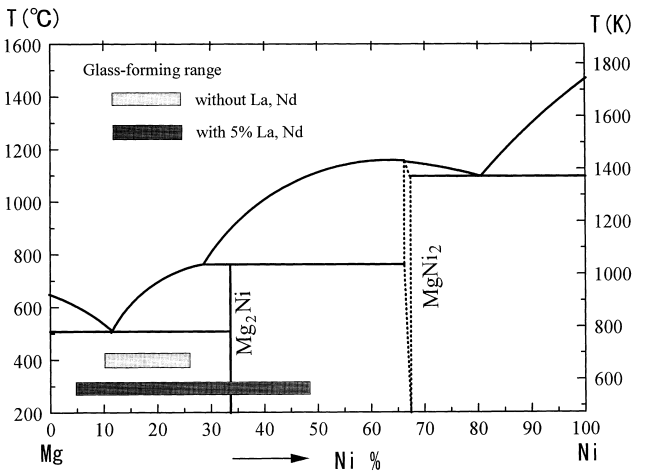

Fig. 1. Phase diagram of the Mg–Ni system including the glass-forming ranges with and without 5 at.% RE.

*Corresponding author.

0925-8388/99/$ – see front matter
PII: S0925-8388(99)00477-6

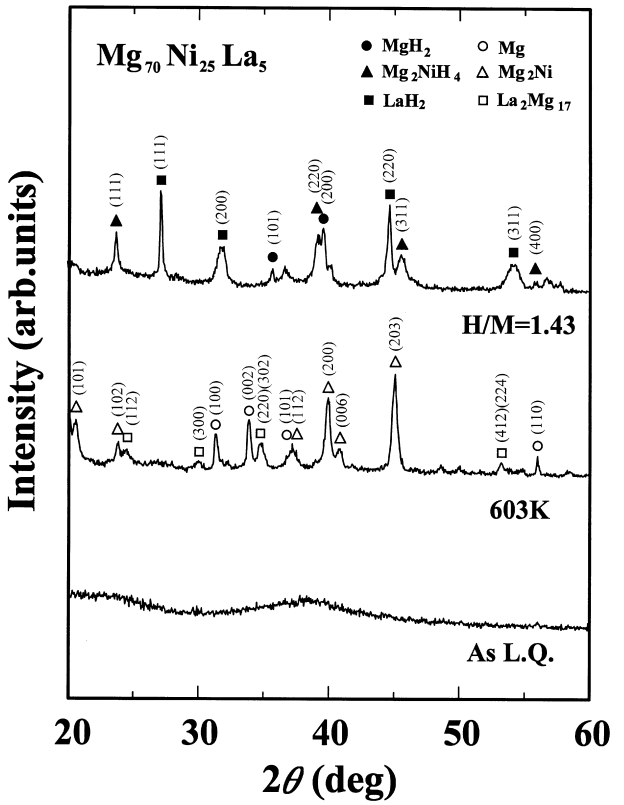

Fig. 2. X-ray diffraction patterns of as melt-spun, melt-spun + crystallized, and melt-spun + crystallized + hydrided $Mg_{70}Ni_{25}La_5$ alloys.

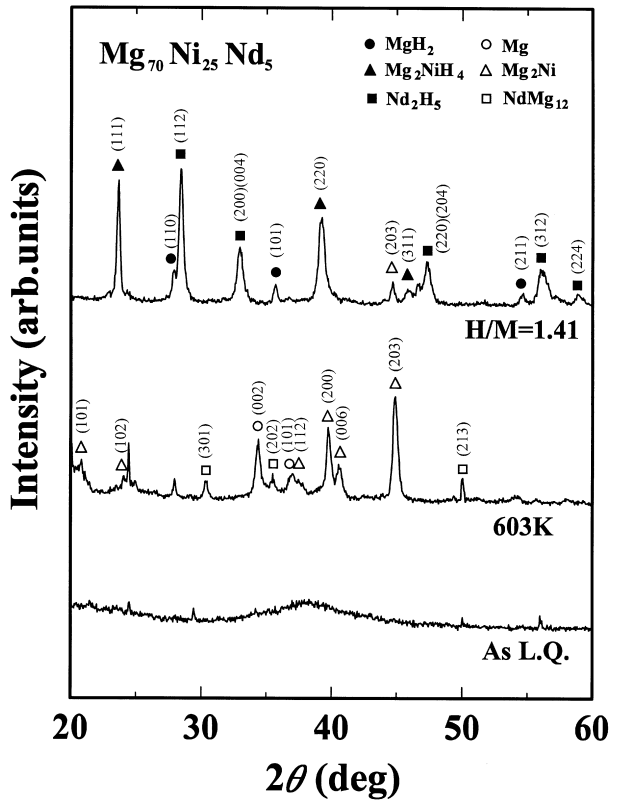

Fig. 3. X-ray diffraction patterns of as melt-spun, melt-spun + crystallized, and melt-spun + crystallized + hydrided $Mg_{70}Ni_{25}Nd_5$ alloys.

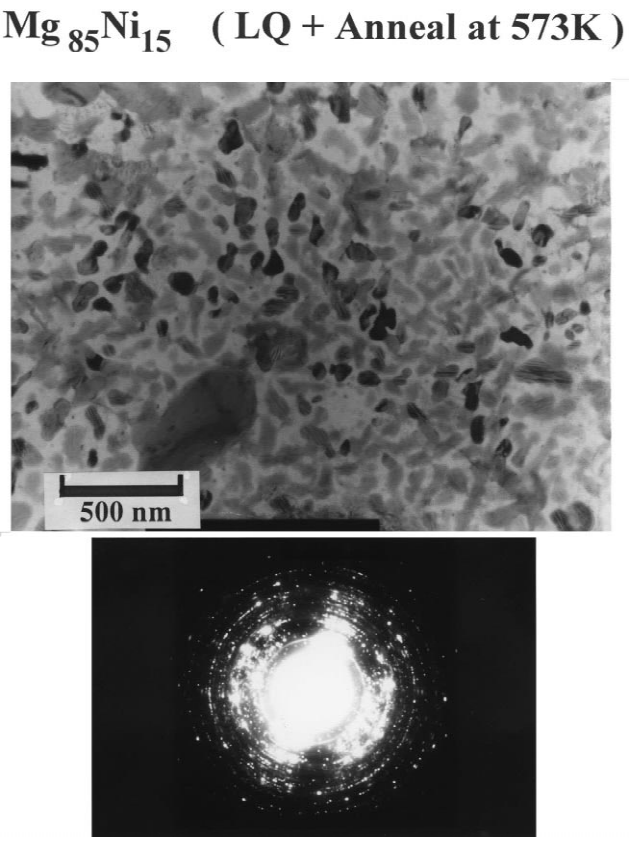

Fig. 4. Transmission electron micrograph and electron diffraction pattern of a melt-spun + crystallized $Mg_{85}Ni_{15}$ alloy.

alloys of various compositions within these ranges, namely, Mg–(15–25)% Ni, Mg–(15–25)% Ni–5% La and Mg–(15–25)% Ni–5% Nd, were prepared by melt-spinning in a form of ~20 μm thick and ~2 mm wide ribbons in Ar atmosphere. Their crystallization temperatures T_x determined by DSC measurements, which mostly displayed doublet exothermic peaks, fell within the range 435±5 K independently of the alloy compositions. The crystallization products as examined by X-ray diffraction were: $Mg + Mg_2Ni$ (for Mg–Ni), $Mg + Mg_2Ni + La_2Mg_{17}$ (for Mg–Ni–La), and $Mg + Mg_2Ni + NdMg_{12}$ (for Mg–Ni–Nd), as shown in Figs. 2 and 3 for the ternary alloys.

Transmission electron micrographs of these crystallized alloys show that they are composed of mixtures of the coexisting phases with grain sizes of 50–100 nm, as shown for $Mg_{85}Ni_{15}$ in Fig. 4. As-cast alloys were also prepared, for comparison, by melt-spinning at very low cooling rates. These nanocrystallized samples were subjected to hydriding (10.8 ks in 3.5 MPa H_2)–dehydriding (3.6 ks in vacuum) treatments at 573–603 K for several cycles, and the hydrogen absorbing–desorbing rates were measured.

3. Results and discussion

Fig. 5 shows the hydriding behavior of $Mg_{85}Ni_{15}$, $Mg_{80}Ni_{15}La_5$ and $Mg_{80}Ni_{15}Nd_5$ alloys at 573 K for the

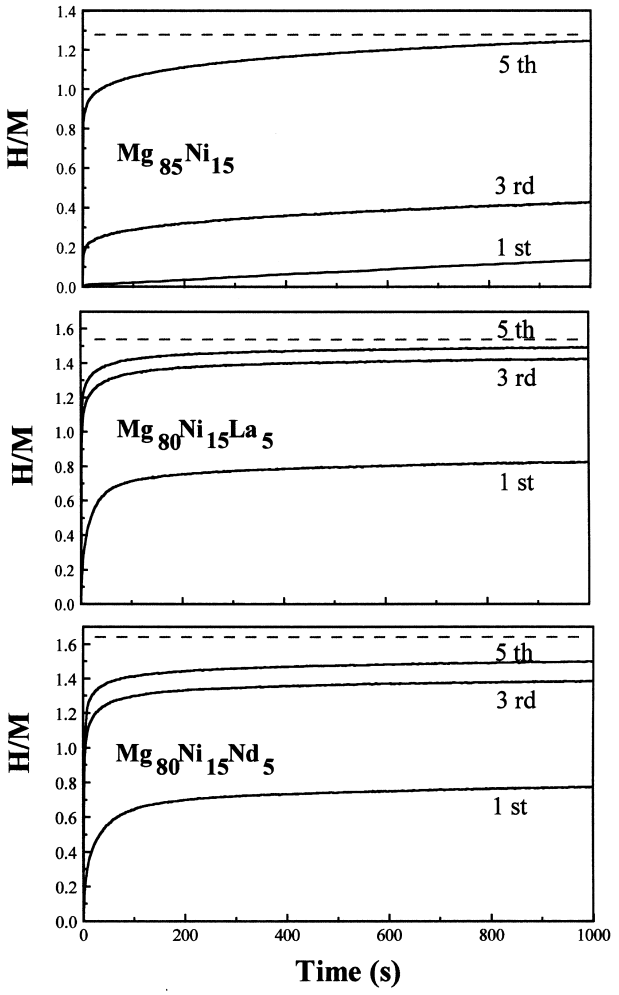

Fig. 5. Hydriding behavior of melt-spun+crystallized $Mg_{85}Ni_{15}$, $Mg_{80}Ni_{15}La_5$ and $Mg_{80}Ni_{15}Nd_5$ alloys under 3.5 Mpa H_2 at 573 K for the first five cycles.

first five cycles; the maximum hydrogen contents attained after hydriding for 10.8 ks are H/M=1.31, 1.54 and 1.62 (dashed lines), respectively. From this figure, we find that the ternary Mg–Ni–RE alloys have good reactivity with hydrogen and can be activated only after the 3rd cycle, compared with the binary Mg–Ni alloy which requires further cycles for the complete activation. We emphasize here that all these nanocrystallized alloys exhibit faster hydriding rates than the corresponding as-cast alloys (not shown in the figure). Fig. 6 shows the hydriding behavior of a completely activated $Mg_{80}Ni_{15}La_5$ alloy at 573, 523 and 473 K. The hydriding rate is appreciably reduced with decreasing temperature. However, the rates at 523 and 473 K were also faster than those of the as-cast alloy.

A similar hydriding behavior was observed for $Mg_{75}Ni_{25}$, $Mg_{70}Ni_{25}La_5$ and $Mg_{70}Ni_{25}Nd_5$ alloys, for which the maximum hydrogen contents attained were H/M=1.25, 1.43 and 1.41, respectively. X-ray diffraction analyses indicate that the following hydriding reactions take place in these alloys, as shown in Figs. 2 and 3:

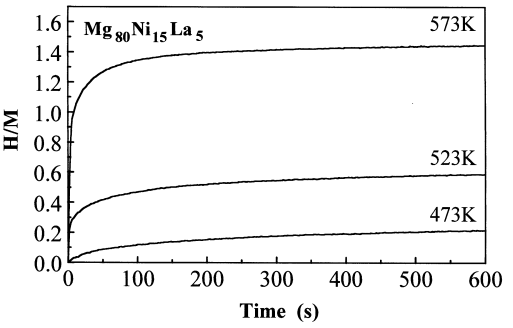

Fig. 6. Comparison of the hydriding behavior of a fully activated $Mg_{80}Ni_{15}La_5$ alloy at 473–573 K.

$Mg \rightarrow MgH_2$, $Mg_2Ni \rightarrow Mg_2NiH_4$, $La_2Mg_{17} \rightarrow LaH_2 + MgH_2$, and $NdMg_{12} \rightarrow Nd_2H_5 + MgH_2$.

Figs. 7 and 8 show *PCT* curves (desorption process) for the $Mg_{80}Ni_{15}Nd_5$ and $Mg_{70}Ni_{25}Nd_5$ alloys, respectively, measured between 553 and 603 K. Both alloys clearly exhibit two-plateau characteristics representing the decompositions of Mg_2NiH_4 (higher plateau) and MgH_2 (lower plateau) hydride phases. The standard enthalpy and entropy changes associated with these decompositions, as evaluated from the plateau pressures, are: $\Delta H^\circ = 69$ kJ/mol H_2 and $\Delta S^\circ = 129$ J/mol $H_2 \cdot K$ for Mg_2NiH_4, and $\Delta H^\circ = 76$ kJ/mol H_2 and $\Delta S^\circ = 136$ J/mol $H_2 \cdot K$ for MgH_2, in reasonable agreement with those reported for the

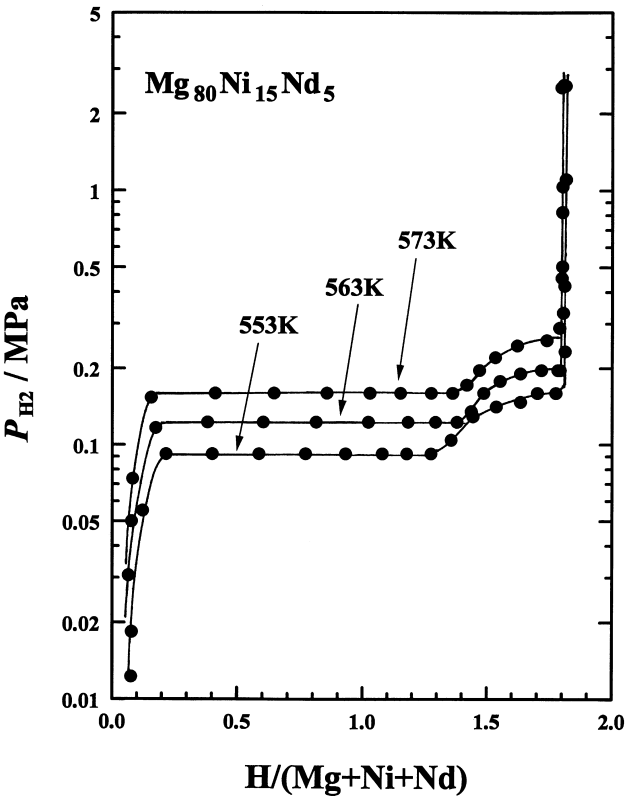

Fig. 7. Pressure–composition isotherms (desorption) of a melt-spun+crystallized $Mg_{80}Ni_{15}Nd$ alloy.

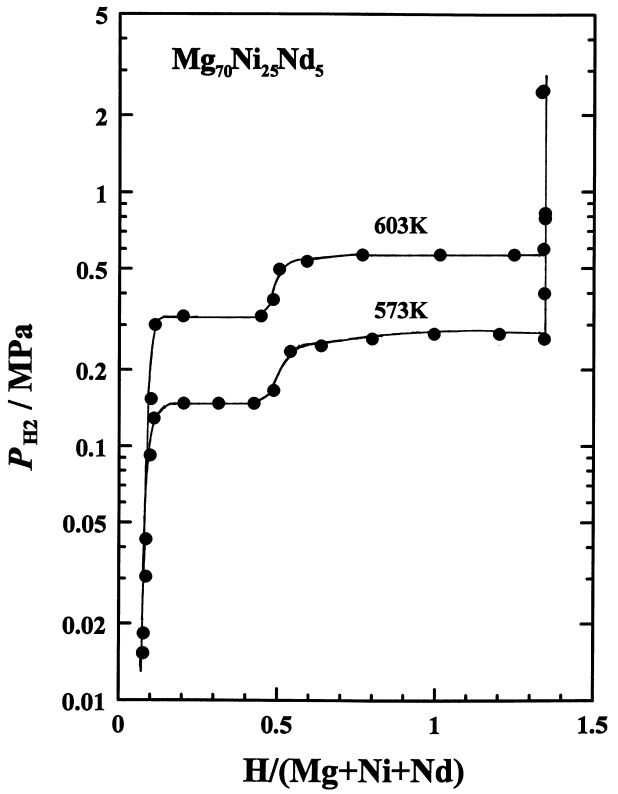

Fig. 8. Pressure–composition isotherms (desorption) of a melt-spun + crystallized $Mg_{70}Ni_{25}Nd$ alloy.

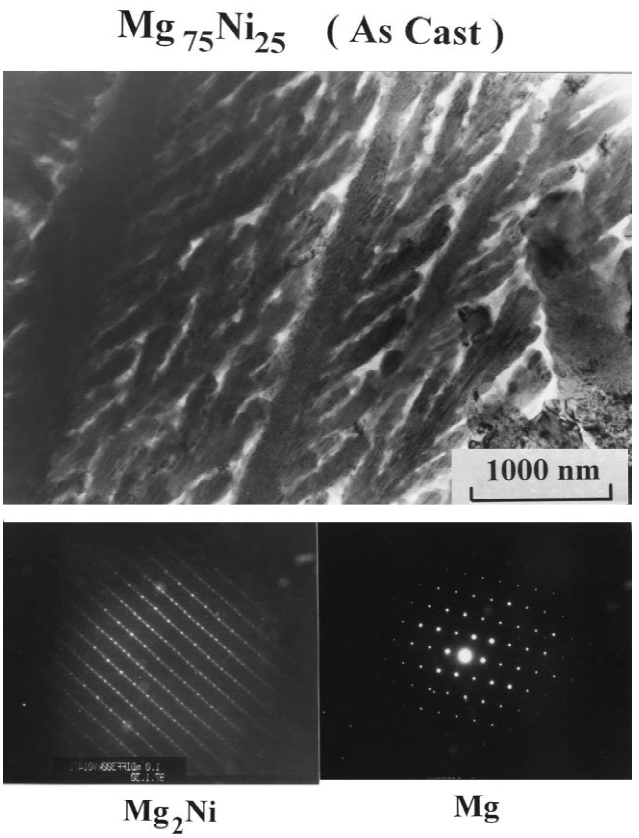

Fig. 9. Transmission electron micrograph and electron diffraction patterns of an as-cast $Mg_{75}Ni_{25}$ alloy.

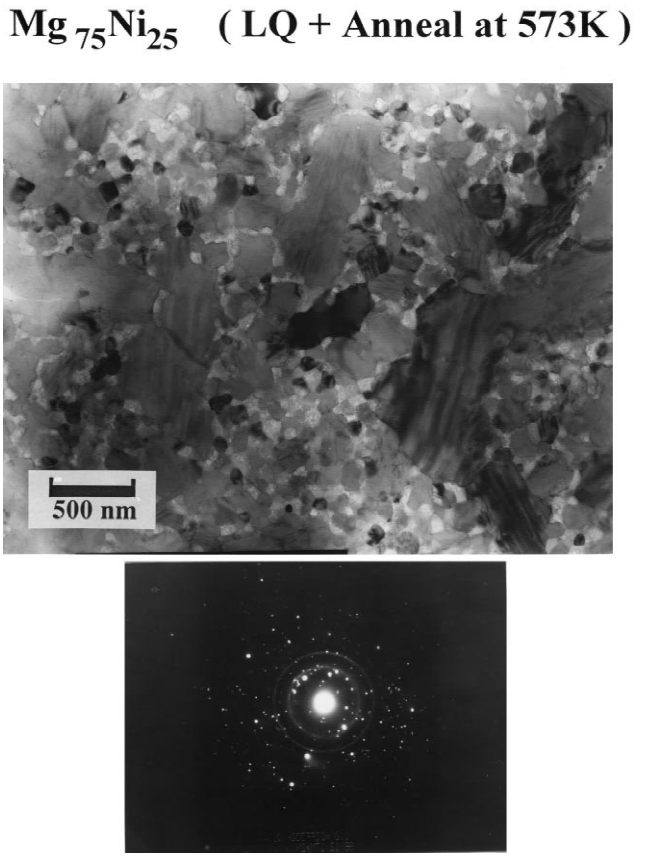

Fig. 10. Transmission electron micrograph and electron diffraction pattern of a melt-spun + crystallized $Mg_{75}Ni_{25}$ alloy.

ordinary monophase materials [3]. The *PCT* characteristics of the Mg–Ni and Mg–Ni–La alloys were similar to those of the Mg–Ni–Nd alloys shown above.

In Figs. 9–11, the microstructures of as-cast, melt-spun + crystallized, and melt-spun + crystallized + hydrided $Mg_{75}Ni_{25}$ alloys observed by TEM are presented, together with their electron diffraction patterns. In the as-cast alloy, a coarse eutectic structure of Mg and Mg_2Ni is seen (Fig. 9), whereas, in the melt-spun + crystallized alloy, nanocrystallized grains (50–100 nm in diameter) of Mg (bright) and Mg_2Ni (dark) are formed, although coarse grains of Mg_2Ni (d~500 nm) with twin fringes are also seen (Fig. 10). This nanocrystalline structure is rather stable and is not much affected by the hydriding to $H/M = 1.4$ after the 5th hydriding–dehydriding cycle (Fig. 11). During these cycles, the coarse grains of Mg_2Ni appear to be partly pulverized into nanocrystalline grains.

The microstructures of the ternary Mg–Ni–RE alloys are currently under investigation, so that direct comparison with the microstructure of the binary Mg–Ni alloy is not possible at the present time. However, the formation of La_2Mg_{17} or $NdMg_{12}$ minor phase upon crystallization (Figs. 2 and 3) is expected to prevent the grain growth of the major phases of Mg and Mg_2Ni, which may cause much finer microstructures in the ternary alloys than in the

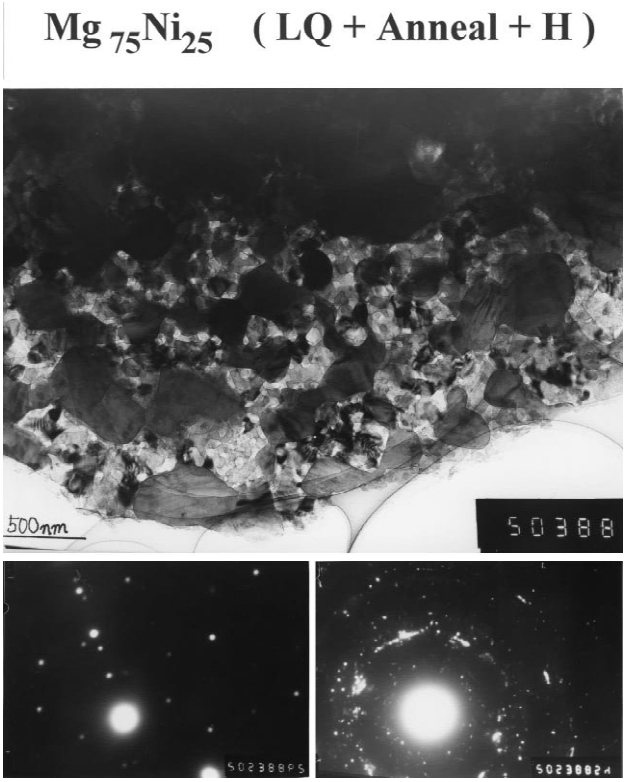

Fig. 11. Transmission electron micrograph and electron diffraction patterns of a melt-spun + crystallized + hydrided $Mg_{75}Ni_{25}$ alloy.

binary alloy and hence enhance the hydrogen reactivity of the ternary alloys.

4. Conclusions

The development of Mg-based alloys with excellent hydriding–dehydriding kinetics is necessary for the future hydrogen energy systems, because they potentially have much greater hydrogen storage capacities per mass than any other materials currently used. The present study shows that the nanocrystallization of melt-spun amorphous alloys of the Mg–Ni–RE systems is one of the prospective approaches for attaining this purpose.

Acknowledgements

This work is partly supported by the Grant-in-Aid for scientific research on priority areas A of new protium function from The Ministry of Education, Science, Sports and Culture of Japan (No. 10148105).

References

[1] K. Tanaka, in: T. Imura, T. Ichinokawa, H. Kawazoe (Eds.), Proc. Spec. Symp. Advanced Materials (SSAM-4), (The Joint Committee for Advanced Materials Research, Nagoya), 1998, p. 59.
[2] M. Hansen, K. Anderko, Constitution of Binary Alloys, 2nd. edn., McGraw-Hill, New York, 1958.
[3] J.J. Reilly, Z. Phys. Chem. Neue Folge 117 (1979) 155.